

# An Ultra-Stable Cu Nanowire under Thermo-Mechanical Loading: A Molecular Dynamic Study

Vijay Kumar Sutrakar<sup>1</sup> and D Roy Mahapatra<sup>2,3</sup>

<sup>1</sup>Mechanical Engineering Design Division, Aeronautical Development Establishment,  
Defence Research and Development Organization, New Thipasandara Post,  
Bangalore, India 560075

<sup>2</sup>Department of Aerospace Engineering, Indian Institute of Science,  
Bangalore, India 560012

## ABSTRACT

We report on the formation of a stable Body-Centered Heptahedral (BCH) crystalline nanobridge structure of diameter  $\sim 1$ nm under high strain rate tensile loading to a  $\langle 100 \rangle$  Cu nanowire. Extensive Molecular Dynamics (MD) simulations are performed. Six different cross-sectional dimensions of Cu nanowires are analyzed, i.e.  $0.3615 \times 0.3615 \text{ nm}^2$ ,  $0.723 \times 0.723 \text{ nm}^2$ ,  $1.0845 \times 1.0845 \text{ nm}^2$ ,  $1.446 \times 1.446 \text{ nm}^2$ ,  $1.8075 \times 1.8075 \text{ nm}^2$ , and  $2.169 \times 2.169 \text{ nm}^2$ . The strain rates used in the present simulations are  $1 \times 10^9 \text{ s}^{-1}$ ,  $1 \times 10^8 \text{ s}^{-1}$ , and  $1 \times 10^7 \text{ s}^{-1}$ . We have shown that the length of the nanobridge can be characterized by larger plastic strain. A large plastic deformation is an indication that the structure is highly stable. The BCH nanobridge structure also shows enhanced mechanical properties such as higher fracture toughness and higher failure strain. The effect of temperature, strain rate and size of the nanowire on the formation of BCH structure is also explained in details. We also show that the initial orientation of the nanowires play an important role on the formation of BCH crystalline structure. Results indicate that proper tailoring of temperature and strain rate during processing or in the device can lead to very long BCH nanobridge structure of Cu with enhanced mechanical properties, which may find potential application for nano-scale electronic circuits.

**Keywords:** Molecular Dynamic, Nanowire, Strain rate, Temperature, Mechanical Properties.

## 1. INTRODUCTION

Metal nanowires are of great technological importance due to their potential applications in nano-scale circuits, optoelectronic and spintronic devices. Nanowires have a large surface area/volume ratio as compared to bulk materials, and their structure and properties can be quite different than those of bulk materials. The structures of ultra thin nanowires of Au [1-6], Cu [7-9], Pb, Al [10-12], Ag [13], and Ti [14] have been investigated using Molecular Dynamics (MD) simulations. These studies show that several helical, multi-shelled, and filled structures exist in several face-centered-cubic (FCC) metals in the form of ultra-thin nanowires. Because of the strong surface effect, unique behaviors such as surface-stress-induced phase transformation [15], lattice reorientation [16-17] have also been observed. Nanowires are of great technological importance because of their unique structures, properties, and potential applications in nanoscale electronics, photonics, biological, and chemical sensors [18-19]. In the recent years, various nano-devices have been developed from nanowires, such as nanolasers [20-21], Field-effect transistors (FET) [22-23], light emitting diode [24], and quantized conductance atomic switch [25].

---

<sup>3</sup> Corresponding Author (D Roy Mahapatra)  
E-mail address: [droymahapatra@aero.iisc.ernet.in](mailto:droymahapatra@aero.iisc.ernet.in)  
Tel: + 91-80-22932419; Fax: +91-80-23600134.

In the previous work on Cu nanowires, atomistic simulations under various conditions have produced many different polygonal cross-section Cu nanowires [9], such as rectangular, pentagonal, and hexagonal ones. Using electron diffraction, high-resolution transmission electron microscopy (HRTEM), and power spectra (PS) results, Lissecki *et al* [26] have shown that a decahedron model explains the structure of the pentagonal Cu nanorods. The coupled effects of geometry and surface orientation of Cu nanowires during mechanical loading at various strain rates and temperature have been analyzed in refs. [27-34]. Mehrez and Ciraci [35] have reported the formation of hexagonal rings by transforming  $\{111\}$  oriented Cu at 150 K. These hexagonal rings further transform into pentagonal rings during mechanical stretching. Sen *et al* [36] have performed an extensive first-principles study of nanowires with various pentagonal structures by using pseudo-potential plane wave method within the framework of density functional theory. They have shown that nanowires of different types of elements, such as alkali, simple, transition, and noble metals and inert gas atoms have a stable structure made of staggered pentagonal shape with a linear chain perpendicular to the planes of the pentagon and passing through their centers. This is due to the fact that the pentagonal quasi-1D nanowires have higher cohesive energy than many other 1D structural arrangements. Recently, Gonzalez *et al* [37] have shown by their experimental and theoretical studies that Cu nanowires formed by mechanical stretching exhibit structural relaxation leading to pentagonal  $[110]$  Cu nanowires with a quantum conductance of  $\sim 4.5 G_0$ . In our recent study [38], we have shown the formation of a stable pentagonal structure under varying strain rate for a temperature of 10K. However, the effects of thermo-mechanical loading on such ultra-thin Cu nanowires on other orientation and size have not been studied. There also exist several possibilities to obtain improved structural stability and improved conductivity with the help of dynamic strain engineering.

In the present paper, we show the reorientation of FCC crystal in a  $\langle 100 \rangle / \{100\}$  Cu nanowire into an ultra-stable pentagonal multi-shell nanobridge structure due to the application of temperature and high strain rate tensile loading. We call the reoriented (transformed) structure as Body-Centered Heptahedral (BCH) crystal since there is a Cu atom at the centre of the crystal and the  $\{100\}$  planes have pentagonal cross-section. The effect of strain rate and temperature on Cu nanowires is also investigated to understand the cause of variations in the structural and mechanical properties. This study shows that the BCH structure has a larger plastic deformation range and they are stable. The effect of initial nanowire orientation on the formation of BCH structure is also discussed. For a given strain rate and temperature, the stability regime of the BCH structure is strongly dependent on the nanowire cross-sectional dimensions. From the results we anticipate various interesting applications of the BCH Cu nanowires, even with diameter as small as  $\sim 1$  nm, in nano-electronic devices.

## 2. SIMULATION

MD simulations of an ultra-thin Cu nanowire are performed using the Embedded Atom Method (EAM). Cu nanowires oriented in the  $\langle 100 \rangle$  direction with a square cross-section and (010) and (001) side surfaces are created using known lattice parameters of a bulk FCC crystal of Cu, as given in Figure 1. In this work, the EAM potential developed by Mishin *et al* [39] is chosen, which accurately represents the elastic properties and the surface energies of copper. More importantly, the potential accurately captures the stacking fault and twinning energies, which is critical in analyzing inelastic deformation. The initial length of the wire is 13 nm with six different cross-sectional dimensions of  $0.3615 \times 0.3615 \text{ nm}^2$ ,  $0.723 \times 0.723 \text{ nm}^2$ ,  $1.0845 \times 1.0845 \text{ nm}^2$ ,  $1.446 \times 1.446 \text{ nm}^2$ ,  $1.8075 \times 1.8075 \text{ nm}^2$ , and  $2.169 \times 2.169 \text{ nm}^2$ . The wires are first relaxed to equilibrium configurations using the conjugate gradient method; they are then thermally equilibrated for a given temperature using the Nose-Hoover thermostat [40, 41] for 10 picosecond (ps) with a time step of 0.001 ps before loading under tension along the wire's axis and is allowed to relax by holding the length of the wire unchanged. The nanowires are not relaxed to a zero stress state and the beginning of deformation under strain rate dependent loading is at a stress level of 1.5 - 8.0 GPa. A similar procedure is also used by Liang and Zhou [42] in the MD simulation during tensile deformation of Cu nanowires. Such an uniaxial loading is performed by completely restraining one end of the wire, and then by applying velocities to the atoms along the loading direction linearly from zero at the fixed end to the maximum value at the free end, creating a ramp velocity profile. Such a ramp velocity is used to avoid the emission of shock waves from the fixed end of the nanowire. The ratio of the peak velocity and the initial length of the nanowire give the strain rate. Three different strain rates of  $1 \times 10^9 \text{ s}^{-1}$ ,  $1 \times 10^8 \text{ s}^{-1}$ , and  $1 \times 10^7 \text{ s}^{-1}$  are used for each nanowire. Simulations are carried out for temperature of 10K, 100K, 200K, 300K, 450K, and 600K. These are done to understand the role of temperature in the formation of BCH structure. The equations of motion are integrated using velocity Verlet algorithm [43]. All simulations are performed using an MD code called LAMMPS [44, 45] developed by Sandia National Laboratory. No periodic boundary conditions were used at any stage of simulation, which is to capture accurately the relevant surface effects. The stresses are calculated using the virial theorem [46]. Engineering strain is used as a measure of deformation and defined as  $(l - l_0)/l_0$ , where  $l$  is the instantaneous length and  $l_0$  is the initial length of the wire obtained after the first step of energy minimization corresponding to the initial configuration. The yield stress and the yield strain are found at the point of initial yield, that is, when the first defect, which typically appears in the

form of a partial dislocation, nucleates within the nanowires. Modulus of elasticity ( $E$ ) is calculated from the initial slope ( $d\sigma/d\varepsilon$ ) of the stress-strain curve for all the cases. The fracture strain is measured at the final breaking point on the stress-strain curve. Fracture toughness ( $\mu$ ) is measured by calculating the area under the stress-strain curve.

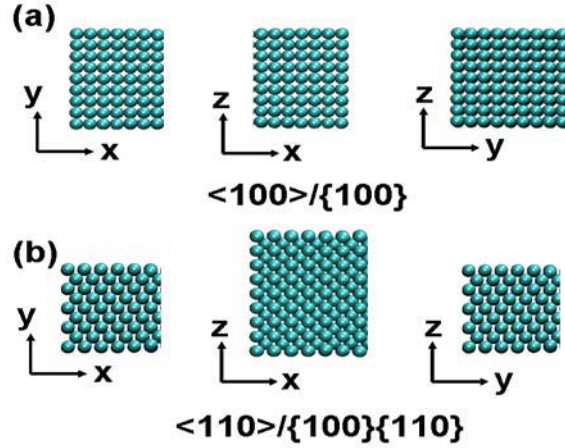


**Figure 1** Cross-sectional views of  $\langle 100 \rangle / \{100\}$  and  $\langle 110 \rangle / \{100\} \{110\}$  Cu nanowires.

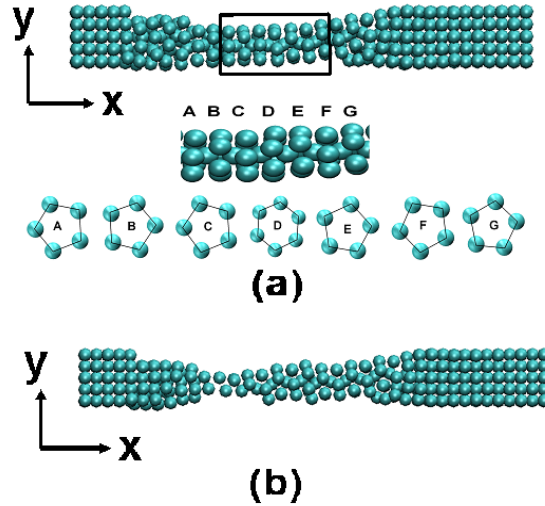


**Figure 2** (a) Formation of pentagon Cu nanowires of  $\langle 100 \rangle$  cross-section at a strain rate of  $1.0 \times 10^9 \text{ s}^{-1}$  and 10 K with few hexahedral ring at the center cross-section. (b) Nanowire just before complete fracture showing a series of stable pentagon Cu lattice.

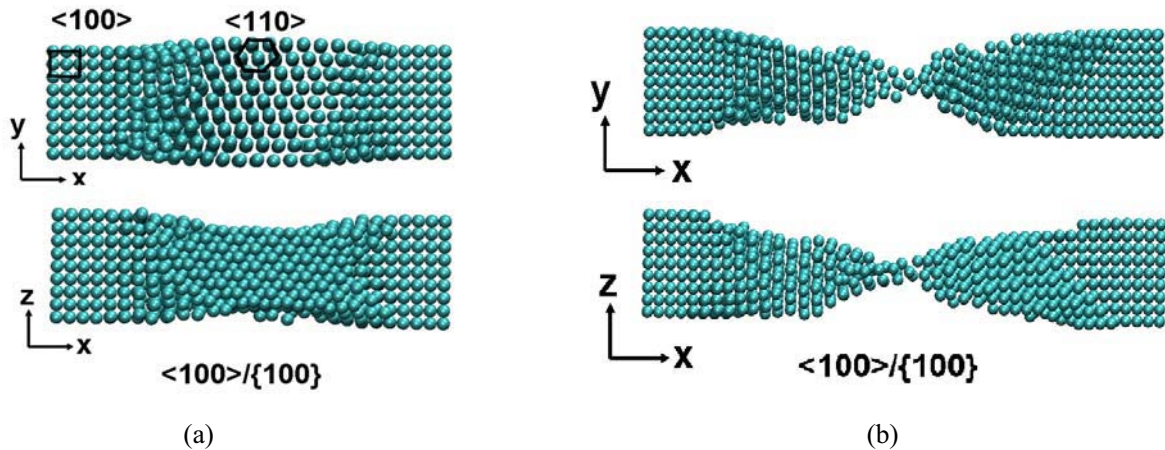
### 3. RESULTS AND DISCUSSIONS

Table 1 shows various cross-sections considered under tensile high strain rate loading of  $1 \times 10^9 \text{ s}^{-1}$  with temperature ranging from 10K-600K. The BCH nanobridge structure is found to be forming for the initial cross-sectional dimensions  $1.8075 \times 1.8075 \text{ nm}^2$  and smaller, whereas our previous studies [35] performed at 10K had shown the formation of the BCH nanobridge structure up-to dimensions  $< 1.5 \text{ nm}$ . This indicates that with proper tailoring of temperature and strain rate, the BCH nanobridge structure can be formed in Cu nanowires of initial cross-sectional dimensions of  $\sim 2 \text{ nm}$ . For a more detailed analysis, a cross-sectional dimension of  $0.723 \times 0.723 \text{ nm}^2$  is considered next. When the nanowire is loaded with a strain rate of  $1 \times 10^9 \text{ s}^{-1}$  at 10K, the BCH nanobridge structure is formed. This structure is obtained via dynamic strain engineering. The structure is illustrated in the snapshot in Figure 2(a).

Portions of the nanobridge are marked with rectangular box and shown in the close-up next to the deformed nanowire snapshots in Figure 2(a). The nanobridge segments are marked as A, B, C, D, E, F, and G and the corresponding sectional views of each of the pentagonal faces are also shown in Figure 2(a). However, because of the high strain rate, the atoms in the square cross-sectional  $\{100\}$  nanowires reorient into  $\{100\}$  pentagonal faces; this is shown in the snapshot in Figure 2(a). A further elongation produces  $\{100\}$  pentagonal face of the BCH structure over several atomic lattices, which is comprised of parallel  $\{111\}$  planes in this particular case of loading, as shown in Figure 2(b). In the present finding, at higher strains due to the applied high strain rate loading, the nanowire becomes unstable and few of BCH crystals are connected by an unstable chain with 1-3 atoms, which forms zigzag pattern in which the atoms move in a helical manner. In several other FCC structures also, such an unstable chain with few atoms are formed before complete fracture of the nanowire, in which the atoms move in a helical, zigzag pattern as observed by Sanchez-Portal *et al* [47] using first principle simulations and by Park and Zimmerman [32] using MD simulations. The onset of the helical, zigzag chain with 1-3 atoms indicates instability in the nanowires, and fracture occurs soon after.

In order to examine the effect of loading rate on the stability of the nanobridge, we analyze the deformation process of a  $0.723 \times 0.723 \text{ nm}^2$  cross-section nanowire loaded with a smaller strain rate of  $1 \times 10^8 \text{ s}^{-1}$  and a temperature of 10K. The above loading condition reorients the structure from  $[100]/\{100\}$  to an atomic thick chain without any crystalline form, which indicates an instability in the nanowires and a further loading causes complete fracture of the structure without any further plastic deformation. To confirm several different behaviors observed in the nanowires of same cross-section with varying strain rates, an even smaller strain rate of  $1 \times 10^7 \text{ s}^{-1}$  and temperature of 10K is applied next. In this case the  $[100]/\{100\}$  Cu nanowire first reorients into a  $\{100\}$  BCH nanobridge structure, and a further loading produces a stable  $\{111\}$  BCH nanobridge structures with unstable thick atom chain in the middle. It shows instability in the nanowires before complete fracture. Non-existence of such BCH nanobridge structures at a strain rate of  $1 \times 10^8 \text{ s}^{-1}$  indicates an exception. This behavior also indicates that large surface-stresses [15] and lateral surface orientations [34] play significant roles in the formation of such stable nanobridge.

It is found that the structure which does not form the pentagons during high strain rate tensile loading of initially  $\langle 100 \rangle$  oriented Cu nanowires, transform into  $\langle 110 \rangle$  orientation during the course of loading. An illustration of such phase transformation from initially  $\langle 100 \rangle$  orientation to  $\langle 110 \rangle$  oriented Cu nanowire under high strain rate tensile loading of  $1 \times 10^9 \text{ s}^{-1}$  and temperature of 10K is shown in Figure 3(a). We have found that the wire with square cross-sectional dimensions less than  $2.0 \times 2.0 \text{ nm}^2$  at a temperature of 10K, which transforms into  $\langle 110 \rangle$  orientation during the course of tensile loading, does not form stable pentagonal nanobridge structure. Figure 3(b) shows the deformed  $\langle 100 \rangle$  initially oriented Cu nanowire just before complete fracture without any formation of stable nanobridge structure having various  $\{110\}$  oriented twin planes. Our study shows that orientation of nanowire has major contribution in the formation of stable nanobridge structure in combination of strain rate, temperature and cross-sectional dimensions.



**Figure 3** (a) Transformation from  $\langle 100 \rangle$  to  $\langle 110 \rangle$  during the high strain rate tensile loading of  $1 \times 10^9 \text{ s}^{-1}$  and temperature of 10K with initial  $1.446 \times 1.446 \text{ nm}^2$  cross-sectional dimension. (b) Initial  $\langle 100 \rangle$  oriented nanowires just before fracture without formation of BCH nanobridge structure.

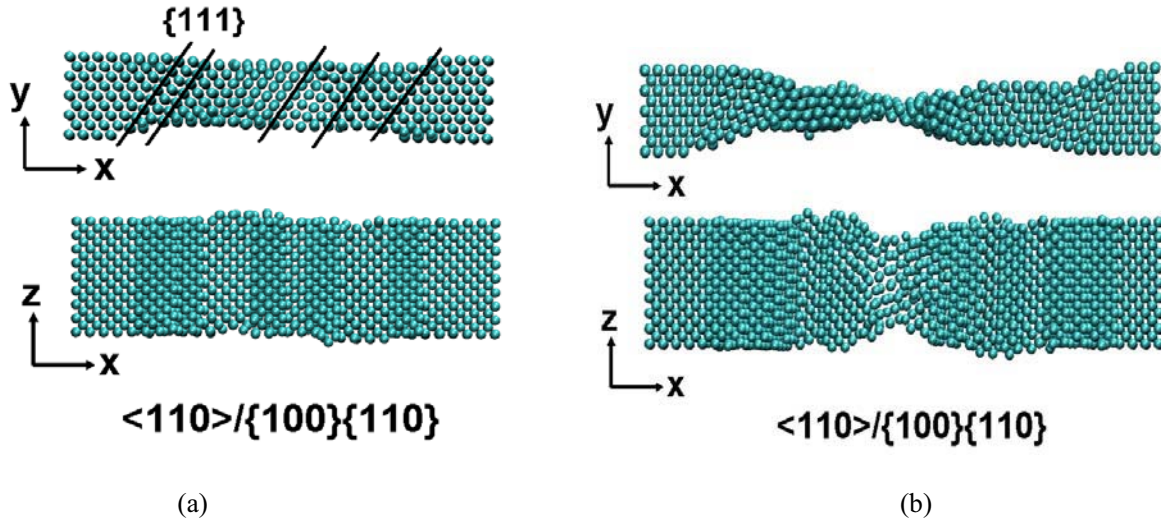


**Figure 4** (a) Formation of  $\{111\}$  slip plane of initially  $\langle 110 \rangle / \{100\} \{110\}$  oriented Cu nanowires during the high strain rate tensile loading of  $1 \times 10^9 \text{ s}^{-1}$  and temperature of 10K with initial  $1.446 \times 1.446 \text{ nm}^2$  cross-sectional dimension. (b) Initial  $\langle 110 \rangle$  oriented nanowires just before fracture without formation of BCH nanobridge structure.

Further, to confirm the non-existence of such stable structure due to transformation of initial  $\langle 100 \rangle$  oriented structure into  $\langle 110 \rangle$  during loading, an initial  $\langle 110 \rangle$  oriented nanowire is created from the bulk FCC Cu. It is found that the initial  $\langle 110 \rangle$  oriented nanowire under high strain rate tensile loading deforms via  $\{111\}$  slip plane without formation of any nanobridge structure. The formation of  $\{111\}$  slip planes of initially  $\langle 110 \rangle / \{100\} \{110\}$  oriented nanowires is shown in Figure 4(a). The  $\langle 110 \rangle$  oriented nanowire just before fracture is shown in Figure 4(b) without any existence of the BCH structure. It confirms that the nanowire orientations and lateral surfaces are also responsible for the formation of the BCH structure.

In order to investigate the effect of temperature on the ultra-thin Cu nanowire, various temperatures of 10K, 100K, 200K, 300K, 450K, and 600K are considered along with the strain rates as considered previously. The deformed Cu nanowires of initial cross-sectional dimensions of  $0.723 \times 0.723 \text{ nm}^2$  under various temperatures ranging from 10K to 600K are shown in Figures 5(a), (b), and (c) for strain rates of  $1 \times 10^7 \text{ s}^{-1}$ ,  $1 \times 10^8 \text{ s}^{-1}$ , and  $1 \times 10^9 \text{ s}^{-1}$ , respectively.

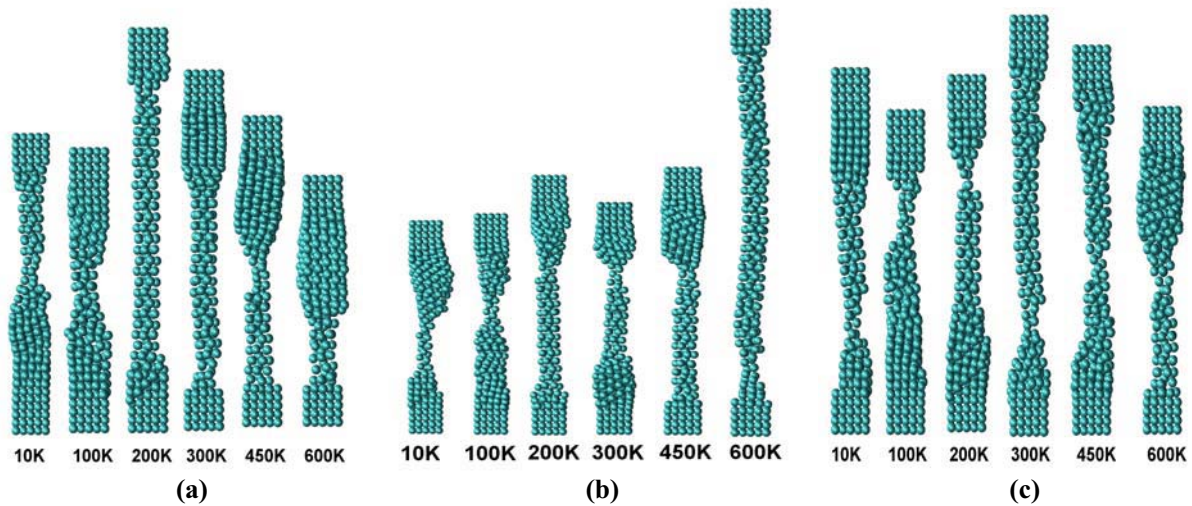


**Figure 5** Snapshot of Cu nanowire with initial cross-sectional dimensions of  $0.723 \text{ nm} \times 0.723 \text{ nm}$  at various temperature ranging from 10K to 600K and under strain rate of (a)  $1 \times 10^7 \text{ s}^{-1}$ , (b)  $1 \times 10^8 \text{ s}^{-1}$ , (c)  $1 \times 10^9 \text{ s}^{-1}$ . The snapshots are taken just before fracture of the nanowires.

Our study shows that some of the nanowires of dimensions even less than 2 nm do not form the BCH nanobridge structures as shown in Figures 5(a) and (b) for temperatures of 100K and 10K and strain rates of  $1 \times 10^7 \text{ s}^{-1}$  and  $1 \times 10^8 \text{ s}^{-1}$ , respectively. Few configurations in Figure 5, which forms the BCH nanobridge structure for a combination of temperature and strain rate, show significant variations in the length of the nanobridge. This indicates that both temperatures as well as strain rate play crucial roles in the formation of such a crystalline nanobridge structure. No direct correlation among the temperature, strain rates, and cross-sectional dimension are found for the present  $\langle 100 \rangle / \{100\}$  Cu nanowire.

Stress-strain curves for all the nanowires with various strain rates and temperature are obtained and quantities like yield stress, yield strain, elastic modulus, plastic strain, and fracture toughness due to formation of the BCH nanobridge are compared. Since the elongation of the nanobridge is significant, it helps in explaining the stability of such a nanowire. Figure 6(a) shows the stress-strain curve for a  $0.726 \times 0.726 \text{ nm}^2$  Cu nanowire for varying strain rates and temperature of 10K. It shows that the initial structure, which transforms into a BCH nanobridge structure, deforms more plastically. Whereas the initial slope of the stress-strain curve is found to be almost constant for a given temperature and cross-sectional dimension with varying strain rate as shown in Figure 6(b). It is observed that for a given temperature and cross-section of the nanowires under varying strain rate, the initial slope of the stress-strain curve (tangent modulus) is constant and hence it is rate insensitive. A decreasing elastic modulus is observed for increasing temperature, which indicates thermal softening due to phase transformation. For a given cross-sectional dimension of the nanowire, the yield stress and the yield strain decrease with increasing temperature for a given strain rate, whereas for a given temperature and cross-sectional dimension with increase in strain rate, one obtains a higher yield stress and a higher yield strain as shown in Figures 6(c) and 6(d), respectively.

In order to analyze the stability of the BCH nanobridge structure, we show the plastic strain and the fracture toughness in Figures 6(e) and 6(f), respectively. It is found that the original structure, which transforms into the BCH nanobridge structure, gives a much larger plastic strain and subsequently higher fracture toughness as compared to a structure, which does not, transform to such a BCH nanobridge structure. For example, the cross-sectional dimension of  $0.723 \times 0.723 \text{ nm}^2$  at temperature of 10K and under a strain rate of  $1 \times 10^7 \text{ s}^{-1}$  and  $1 \times 10^9 \text{ s}^{-1}$  transforms to the BCH nanobridge structure, whereas no such transformation is observed under a strain rate of  $1 \times 10^8 \text{ s}^{-1}$ . Plastic strains of 0.4287 and 0.4972 are obtained for a strain rate of  $1 \times 10^7 \text{ s}^{-1}$  and  $1 \times 10^9 \text{ s}^{-1}$ , respectively, whereas a plastic strain of 0.278 is observed for a strain rate of  $1 \times 10^8 \text{ s}^{-1}$ . Similarly, higher fracture toughness of 4.0824 and 4.9017  $\text{GJ/m}^3$  is observed at a strain rate of  $1 \times 10^7 \text{ s}^{-1}$  and  $1 \times 10^9 \text{ s}^{-1}$ , respectively, whereas 2.535  $\text{GJ/m}^3$  is observed at a strain rate of  $1 \times 10^8 \text{ s}^{-1}$ . The above results indicate that the BCH nanobridge structure deforms more plastically and give higher plastic strain and fracture toughness compared to other forms of Cu, hence such a structure is more stable. It is also observed that the structure which deforms most, gives highest plastic strain of  $\sim 1.18$  for a strain rate of  $1 \times 10^8 \text{ s}^{-1}$  and temperature of 600K as shown in Figure 6(f), and correspondingly the largest length as shown in Figure 5(b). In order to investigate the role of various cross-sectional dimensions on the formation of the BCH nanobridge structure, next we consider six different cases of cross-sectional areas:  $0.3615 \times 0.3615 \text{ nm}^2$ ,  $0.723 \times 0.723 \text{ nm}^2$ ,  $1.0845 \times 1.0845 \text{ nm}^2$ ,  $1.446 \times 1.446 \text{ nm}^2$ ,  $1.8075 \times 1.8075 \text{ nm}^2$ , and  $2.169 \times 2.169 \text{ nm}^2$ . Results show that the nanowires with cross-sectional dimensions only  $< 2.0 \text{ nm}$  reorients from  $[100] / \{100\}$  FCC to stable  $\{111\}$  BCH nanobridge structure, whereas the nanowires with larger dimensions fails mainly by full or partial dislocation via twinning.

#### 4. CONCLUSIONS

In summary, we have reported a stable lattice structure having a body-centered heptahedral (BCH) crystals under high strain rate tensile loading on a  $[100] / \{100\}$  square cross-sectional Cu nanowire. Existence of such a stable structure via transformation of  $\langle 110 \rangle$  oriented Cu nanowire for  $\sim 1 \text{ nm}$  is not observed. It is shown how a strain rate loading can give rise to the stable BCH at various temperature and smaller geometries. Such a stable structure has enhanced mechanical properties, such as higher plastic strain and subsequently higher fracture toughness. From these results, we anticipate several future applications of this type of BCH nanobridge structure of Cu with diameter of  $\sim 1 \text{ nm}$  in nano-electronic devices. In addition, the BCH nanobridge structures are found to have an inherent stability although strongly dependent on temperature and the external loading rate applied to the nanowires. The formation of stable BCH nanobridge structure has been observed for cross-sectional dimensions  $< 2 \text{ nm}$  whereas the nanowires  $> 2 \text{ nm}$  shows failure due to partial or full dislocation via twinning. Strain rate insensitive and cross-sectional dimension insensitive elastic modulus for a given temperature is also found. Decreasing yield stress and yield strain have been observed with decreasing strain rate for a given initial cross-sectional dimensions of the nanowires. For a given strain rate with increasing cross-sectional area, a decreasing yield stress and a decreasing yield strain are also observed. Our studies also show that the length of the BCH nanobridge structures can be

characterized by plastic strain. Proper tailoring of the process temperature and strain rate can be used to form very large BCH nanobridge structure with enhanced mechanical properties.

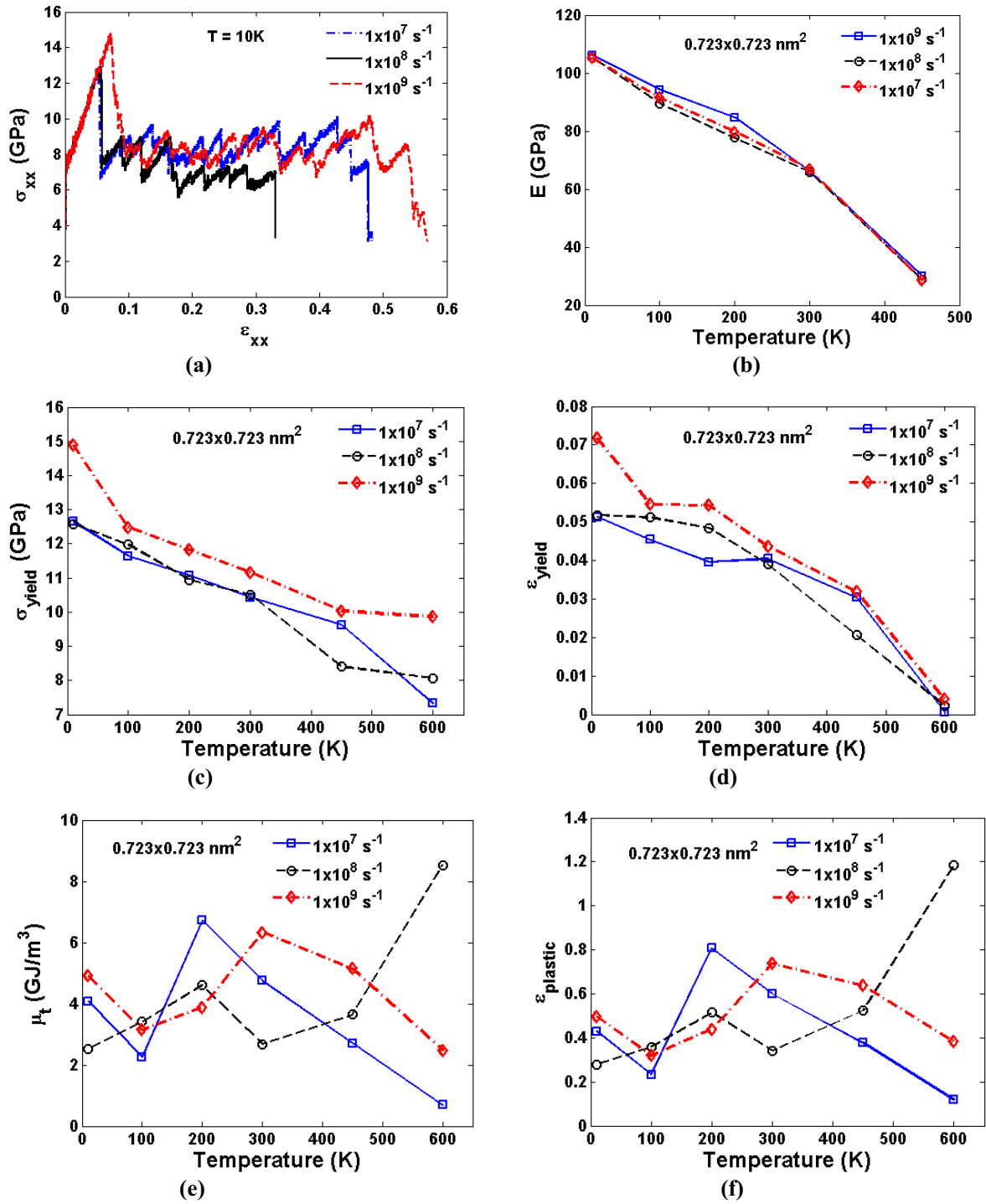


**Figure 6** (a) Stress-strain curve with varying strain rate at 10K, (b) elastic modulus, (c) yield stress, (d) yield strain, (e) fracture toughness, and (f) plastic strain; with varying temperatures and strain rates. Initial cross-sectional dimension of the nanowire is  $0.723 \times 0.723 \text{ nm}^2$ .

## ACKNOWLEDGEMENTS

Vijay Kumar Sutrakar thanks R. Raghunathan, Group Director, and C.M. Venkatesh, Head of Mechanical Engineering Design Division, Aeronautical Development Establishment, Bangalore for their positive support and encouragement during this research work.

## REFERENCES

- [1] Wang B, Yin S, Wang G, Buldum B and Zhao J 2001 *Phys. Rev. Lett.* **86** 2046
- [2] Bilalbegovic G 1998 *Phys. Rev. B* **58** 15 412
- [3] Tosatti E, Prestipino S, Kostlmeier S, Dal Corso A and Di Tolla F D 2001 *Science* **291** 288
- [4] Bilalbegovic G 2000 *Solid State Commun.* **115** 73
- [5] Torres J A, Tosatti E, Dal Corso A, Ercolessi F, Kohanoff J J, Di Tolla F D and Soler J M 1999 *Surf Sci.* **426** L441
- [6] Bilalbegovic G 2000 *Comput. Mater Sci.* **18** 333
- [7] Hwang H J and Kang J W 2002 *J. Korean Phys. Soc.* **40** 283
- [8] Kang J W and Hwang H J 2002 *Mol. Simul* **28** 1021
- [9] Kang J W and Hwang H J 2002 *J. Phys.: Condens. Matter* **14** 2629-2636
- [10] Gulseren O, Erolessi F and Tosatti E 1998 *Phys. Rev. Lett.* **80** 3775
- [11] Di Tolla F, Dal Corso A, Torres J A and Tosatti E 2000 *Surf Sci.* **456** 947
- [12] Gulseren O, Erolessi F and Tosatti E 1995 *Phys. Rev. B* **51** 7377
- [13] Finbow G M, Lyden-Bell R M and McDonald I R 1997 *Mol. Phys.* **92** 705
- [14] Wang B, Yin S, Wang G and Zhao J 2001 *J. Phys.: Condens. Matter* **13** L403
- [15] Diao J and Gall K 2003 *Nature Materials* **2** 656-660.
- [16] Kondo Y and Takayanagi K 1997 *Phys. Rev. Lett.* **79** 18
- [17] Diao J and Gall K 2004 *Phys. Rev. B* **70** 075413
- [18] Lieber C M 2003 *MRS Bulletin* **28** 7
- [19] Patolsky F and Lieber C M 2005 *Materials Today* **8** 4
- [20] Huang M H and Mao S 2001 *Science* **292** 5523
- [21] Dual X and Huang Y 2003 *Nature* **421** 241-245
- [22] Arnold M S and Avouris P 2003 *J Phys. Chem. B.* **107** 659-663
- [23] Wu Y and Xiang J 2004 *Nature* **430** 61-64
- [24] Duan X and Hunag Y 2003 *Nature* **409** 66-69
- [25] Terabe K and Hasegawa T 2005 *Nature* **433** 47-50
- [26] Lisiecki I, Filankembo A, Sack-Kongehi H, Weiss K, Pilemi M P and Urban J 2000 *Phys. Rev. B* **61** 4968
- [27] Liang W, Tomer V and Zhou M 2003 *Nanowires and Nanobelts: Materials, properties and Devices.* ZL Wang, New York, Springer 122-155
- [28] Liang W and Zhou M 2004 *J Mech Engg Sci.* **218** 6
- [29] Liang W and Zhou M 2005 *J Engg Mater. And Tech.* **127** 4
- [30] Liang W and Zhou M 2006 *Phys. Rev. B* **73** 115409
- [31] Liang W and Zhou M 2005 *Nano Lett.* **5** 10
- [32] Park H S, Gall K and Zimmerman J A 2005 *Phys. Rev. Lett.* **95** 255504
- [33] Changjiang Ji and Harold S Park 2006 *Appl.Phys.Lett* **89** 181916
- [34] Changjiang Ji and Harold S Park 2007 *Nanotechnology* **18** 305704
- [35] Mehrez H and Ciraci S 1997 *Phys. Rev. B* **56** 12632
- [36] Sen P, Gulseren O, Yildirim T, Batra IP, and Ciraci S 2002 *Phys. Rev. B* **65** 235433-1
- [37] Gonzalez JC, Rodrigues V, Bettini J, Rego LGC, Rocha AR, Coura PZ, Dantas SO, Sato F, Galvao DS, and Ugarte D 2004 *Phys. Rev. Lett.* **93** 126103-1
- [38] Sutrarak Vijay Kumar and Mahapatra D Roy 2008 *J. Phys.: Condens. Matter* (Accepted Manuscript)
- [39] Mishin Y, Mehl M, Papaconstantopoulos D A, Voter A F and Kress J D 2001 *Phys. Rev. B* **63** 224106
- [40] Nose S 1984 *J Chem Phys.* **81** 511-9
- [41] Hoover W G 1985 *Phys. Rev. A* **31** 1695-7
- [42] Liang W and Zhou M 2003 *Nanotech* **2**, [www.nsti.org](http://www.nsti.org), ISBN 0-9728422-1-7
- [43] Swope W C, Anderson H C, Berens P H, and Wilson K R 1982 *J Chem Phys.* **76** 637-649
- [44] Plimpton S J 1995 *J Comput. Phys.* **117** 1-19
- [45] LAMMPS 2007 <http://www.cs.sandia.gov/~sjplimp/lammps.html>
- [46] Zhou M 2003 *Proc. R. Soc. A* **459** 2347-92
- [47] Sanchez-Portal D, Artacho E, Junquera J, Ordejon P, Garica A and Soler J M 1999 *Phys Rev Lett* **83**(19):3884-7